Acoustic Tag State Estimation with Unsynchronized Hydrophones on AUVs

Jingnan Shi[1], Tianyi Ma[1], Chi-Yen Lee[1], Eyassu Shimelis[1],
Charles Van Eijk[1], Christopher G. Lowe[2] and Christopher M. Clark[1]

***Abstract*— This paper presents an underwater robotic sensor system for localizing acoustic transmitters when the robot's hydrophones can not be time-synchronized. The development of the system is motivated by applications where tracking of marine animals that are tagged with an underwater acoustic transmitter is required. The system uses two novel real-time calibration algorithms that improve the accuracy of time of flight (TOF) and time difference of arrival (TDOA) measurements. The first algorithm corrects non-linear clock skews in TOF measurements based on temperature variation. The second algorithm compensates the localized relative clock skew between clocks using a mixed integer linear program. To validate the system's performance, an Autonomous Underwater Vehicle (AUV) was deployed to track a moving tag where GPS data was used as ground truth. Compared to traditional TOF and TDOA filtering methods, the results show that the proposed system can achieve reduction of mean localization errors by 59%, and a reduction of the standard deviation of measurements by 44%.**

I. Introduction

Tracking movement behaviors of marine animals is a necessary component for understanding underwater ecosystems. Typical methods for tracking marine animals includes physically tagging them with acoustic transmitters, and using hydrophone-receiver systems to receive the transmitted acoustic signals. Recent research has shown that such hydrophone receiver systems can be implemented on autonomous underwater vehicles (AUVs) or even multi-AUV systems, tasked with actively tracking fish or sharks [1]–[3].

Within AUV tracking systems, and particularly multi-AUV systems, the clocks on the different hydrophone-receivers must be synchronized for extracting the accurate time of flight (TOF) and time difference of arrival (TDOA) values necessary for obtaining range-to-tag and bearing-to-tag measurements. Unfortunately, clocks of different hydrophone-receivers are subject to temperature-induced clock drifts and a lack of clock synchronization [4].

This paper offers a solution to the drift problem by presenting an AUV localization system that is capable of performing real-time calibration. It corrects non-linear clock drift in real-time to produce accurate TOF data. In addition, the system leverages known physical parameters of the hydrophone-receiver system to compensate relative clock skew between hydrophones, and calculate TDOA measurements. The TOF and TDOA data are used to produce range and bearing measurements, which are then fed into a particle filter for target state estimation. To validate performance, this paper examines an unsynchronized hydrophone-receiver pair in an AUV tracking system. This system consists of an OceanServer Iver2 AUV, two VR2C 69 kHz hydrophones that are attached to both ends of the AUV, and a 69 kHz Vemco V9 periodic acoustic transmitter tag (see Fig. 1). Each hydrophone receiver is bundled with microprocessors that process acoustic data individually. The hydrophones are configured to send timestamps of received signals with microsecond resolution, as well as measured temperatures to the Iver2 AUV computer via serial communication.

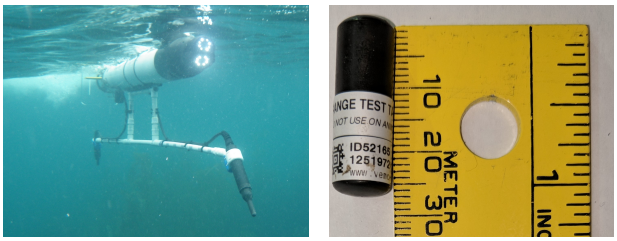

(a) (b)

Fig. 1: (a) shows the OceanServer Iver2 equipped with two hydrophone-receivers; (b) shows a Vemco 69 kHz V9 acoustic tag.

The contributions of this work include:

1) An algorithm that dynamically compensates for non-linear clock drift in TOF calculations based on temperature variations.
2) An algorithm that uses a mixed integer linear programming (MILP) formulation to perform regression to estimate the skew between clocks to obtain TDOA measurements.
3) A full system verification of localizing tagged objects using the purposed system.

Two experimental data sets are used to validate the system. In these experiments, localization of a tagged moving target was conducted at Big Fisherman's Cove, Santa Catalina Island, during August of 2017.

The paper is organized in the following manner: Section II describes relevant past work. Section III, IV, V and VI describe details of the proposed system, including the algorithm developed for correcting non-linear clock drift, the algorithm and MILP formulation developed for estimating relative clock drift between hydrophones dynamically, and the particle filter used for estimating the position of the

[1] Dept. of Engineering, Harvey Mudd College, Claremont, CA 91711 jshi@, tma@, johlee@, eshimelis@, cvaneijk@, clark@hmc.edu

[2] Department of Biological Sciences, CSU Long Beach, Long Beach, CA 90840 clowe@csulb.edu

target. Section VII presents the experiments performed and results. Conclusions and future work are presented in Section VIII.

II. Background

Underwater localization of acoustic tags is a well researched field [5]–[8]. Localization is achieved through algorithms based on TOF, TDOA, signal amplitude or any combination of the three. Using Radio Signal Strength Indicator (RSSI) detection, Hook et al. investigated strategies to localize fish [9]. Shatara and Tan presented an efficient TOF-based algorithm to localize small robotic fish within a sensor array [10]. Lin et al. proposed an algorithm that localizes acoustic tags using TOF measurements obtained from two synchronized hydrophones on an AUV [1]. Espinoza et al. described and tested a new acoustic telemetry system that can accurately localize aquatic animals using a 3-receiver TDOA algorithm [11].

These localization algorithms rely on accurate TOF and TDOA measurements. To obtain such measurements, one can build a hydrophone array with a data acquisition module (DAQ), and use a high-accuracy clock such as a SA.45s chip scale atomic clock (CSAC) to synchronize all hydrophones [8]. The obtained acoustic data can then be processed with algorithms such as matched filtering and phased-array beamforming. However, the costs and efforts involved in building such systems might be prohibitive.

Instead of implementing such custom systems, one may choose to use off-the-shelf hydrophone receivers produced by companies like Vemco. Such hydrophones can usually be configured to output timestamps when signals from acoustic tags are received. To calculate TOF and TDOA measurements, one needs to synchronize the hydrophones. However, high-resolution synchronization between these hydrophones is difficult, if not impossible: Vemco hydrophone clocks can be synchronized with PC clocks with an accuracy of only 1 second [12]. In addition, the crystal oscillators in the hydrophones are subject to drifts caused by changes in temperature, and the hydrophone clocks will become unsynchronized during operation [13]. One method to correct clocks drifts is to periodically synchronize hydrophones with GPS time [14]. However, GPS signals are unavailable while vehicles are underwater.

The impact of hydrophone clock drift is insignificant in large-scale array systems in which unsynchronized hydrophones are separated by hundreds or thousands of meters. In [4], Warnar and Hannay utilized and tested a TDOA based algorithm to localize bowhead whales. In their system, clock drift was insignificant since the separation between hydrophones was large. However, the separation between hydrophones on common AUV systems is on the order of meters, or even centimeters [1], [8]. The influence of clock drift becomes more prominent for such small separations.

Previous research has been conducted to specifically compensate for clock drift to achieve better localization accuracy. In [15], a linear model is used to estimate clock drifts, but is only valid under a constant temperature environment. In [16], quadratic regression is used to compensate the drift of a quartz clock and reduces the localization error from about one thousand meters to three hundred meters. Unlike these previous works, proposed here are two novel algorithms that compensate for non-linear clock drifts between multiple hydrophones that are not time-synchronized.

III. Tag Position State Estimation System Overview

The acoustic tag state estimation system presented in this paper has three parts. First, the system estimates the TOF from the AUV to the acoustic tag with a temperature-based dynamic clock skew estimation algorithm. The TOF is used to calculate the distance d between the AUV and the acoustic tag, (see d in Fig. 2). Second, the system estimates TDOA between the two hydrophones with an algorithm that uses a MILP formulation. The TDOA is used to calculate the bearing α between the AUV and the acoustic tag, (see α in Fig. 2). Third, a particle filter fuses the distance and bearing estimates to produce estimates of the tag's positions. Together with position and heading (see γ in Fig. 2) of the AUV, the acoustic tag's global position can be determined.

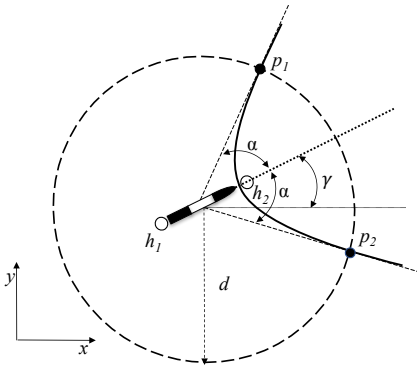

Fig. 2: Illustration of the localization scheme used in this paper. A hyperbola is constructed with TDOA measurement from hydrophone h_1 and h_2. From TOF measurement, a circle of range d can be constructed, and its intersection p_1 and p_2 with the hyperbola represents the two potential locations of the target. Angle α and γ represent the AUV's relative bearing to the target and heading respectively.

IV. Temperature-based Dynamic Clock Skew Estimation for Time-of-flight Distance Estimation

When AUVs are deployed into water, rapid temperature changes can occur and alter the clock speeds on different hydrophones, inducing differences in time measurements [13]. The clock skew is defined as the instantaneous difference between a clock and the true time. The rate at which the clocks drift with respect to the real time is defined as the drift rate. The drift rates might be constant, which will lead to linear clock skew with respect to time, or time-varying, which will lead to non-linear clock skew. The progression of clock timing can be represented by plots such as Fig.

3, where the x-axis represents the true time and y-axis represents the time measured by clocks.

Consider a hydrophone with a non-linear clock skew function and a stationary acoustic tag with a fixed true period. The period of the tag as measured by the hydrophone will be non-constant.

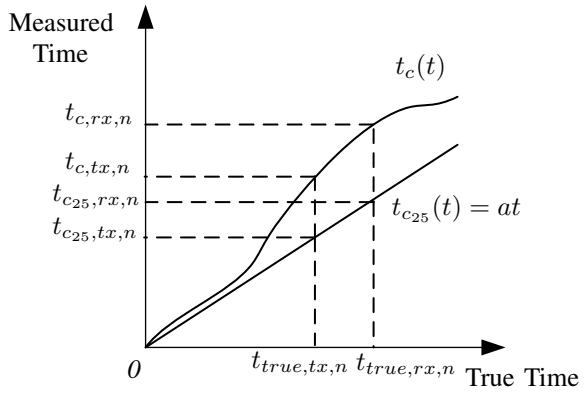

Fig. 3: $t_c(t)$ represents the hydrophone clock with a non-linear clock skew function. $t_{c_{25}}(t)$ represents the linear clock skew function of the imaginary hydrophone clock at 25°C. $t_{true,tx,n}$ and $t_{true,rx,n}$ represent the true transmit and receive times of the n^{th} acoustic signal, $t_{c_{25},tx,n}$ and $t_{c_{25},rx,n}$ represent the measured transmit and receive times on the virtual 25°C clock for this signal, and $t_{c,tx,n}$ and $t_{c,rx,n}$ represent the measured transmit and receive times on the actual hydrophone clock for this signal.

Traditional methods to calculate TOF assuming constant tag periods [2] will accumulate significant error over time. What's more, since it is impossible to measure true times, it is impossible to calibrate the hydrophone beforehand to obtain a function that relates the clock drift rate with respect to a perfect clock. However, a calibration with respect to a virtual clock that represents the hydrophone clock at a constant temperature can be performed. Assuming clock skew depends only on temperature, this virtual clock will have a linear clock skew function. TOF calculations can then be carried out using the methods described in [2].

Such calibration requires knowing the relative drift rate between the non-linear clock and the virtual clock. This allows the function of relative drift rate with respect to temperature to be measured before experiments. In the system implemented in this paper, the temperature of the virtual clock is set to be at 25°C.

A. Linearizing A Non-linear Hydrophone Clock

In this section, time instances are denoted with a three-subscript scheme: $t_{k,x,n}$. The first subscript k indicates whether the time is measured with an actual hydrophone clock (c), the virtual 25°C hydrophone clock (c_{25}), or the perfect clock ($true$). The second subscript x indicates if the time is associated with acoustic signal transmission (tx) or reception (rx). The third subscript n denotes the signal number, e.g. it was the n^{th} signal transmitted. Fig. 3 shows the actual hydrophone clock function $t_c(t)$ together with the virtual linear clock function $t_{c_{25}}(t)$.

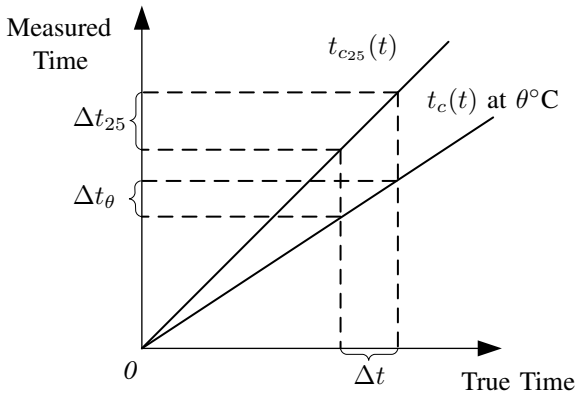

Fig. 4: $t_c(t)$ represents $t_c(t)$ at θ°C. $t_{c_{25}}(t)$ represents $t_c(t)$ at 25°C.

It follows that

$$t_{c_{25},rx,n} = \int_0^{t_{true,rx,n}} \frac{dt_{c_{25}}}{dt} dt \tag{1}$$

Performing substitution of variable with $dt_c = dt\frac{dt_c}{dt}$, Eq. (1) becomes

$$t_{c_{25},rx,n} = \int_0^{t_{c,rx,n}} \frac{dt_{c_{25}}}{dt_c} dt_c \tag{2}$$

Eq. (2) can then be approximated using a discretization

$$t_{c_{25},rx,n} = \sum_{i=0}^{N} \left.\frac{dt_{c_{25}}}{dt_c}\right|_{t=i\Delta t_c} \Delta t_c \tag{3}$$

where N is a positive integer representing the number of discretization intervals, and $\Delta t_c = t_{c,rx,n}/N$. The greater N is, the more accurate Eq. 3 becomes. Since drift rates are dependent on temperature only, it follows that Eq. 3 can be rewritten as

$$t_{c_{25},rx,n} = \sum_{i=0}^{N} g(\theta(i\Delta t_c))\Delta t_c \tag{4}$$

where $g(\theta(t)) = \frac{dt_{c_{25}}}{dt_c}(\theta(t))$ is the relative drift rate function with respect to temperature $\theta(t)$, a function of time.

B. Determining Relative Drift Rates

To determine $g(\theta)$, notice that

$$g(\theta) = \frac{dt_{c_{25}}}{dt_c}(\theta) = \frac{\frac{dt_{c_{25}}}{dt}}{\frac{dt_c}{dt}(\theta)} \tag{5}$$

As shown in Fig. 4,

$$\frac{dt_{c_{25}}}{dt} = \frac{\Delta t_{25}}{\Delta t} \tag{6}$$

$$\frac{dt_c}{dt}(\theta) = \frac{\Delta t_\theta}{\Delta t} \tag{7}$$

Thus,

$$\frac{\frac{dt_{c_{25}}}{dt}}{\frac{dt_c}{dt}(\theta)} = \frac{\Delta t_{25}}{\Delta t_\theta} \tag{8}$$

Using a fixed period acoustic signal transmitter, together with a temperature controlled water bath, $g(\theta)$ can be approximated experimentally with Eq. (8). Δt_θ will be the period of the acoustic tag measured at temperature θ, and Δt_{25} will be the period of the acoustic tag measured at $25°$C.

C. TOF Calculation

With $g(\theta)$ obtained, Eq. 3 can be used to calculate TOF for each signal received. As described in [2],

$$\begin{aligned} \text{TOF}_{c_{25}} &= t_{c_{25},rx,n} - t_{c_{25},tx,n} \\ &= t_{c_{25},rx,n} - (t_{c_{25},tx,0} + kT_{c_{25}}) \end{aligned} \tag{9}$$

where $k = n - 1$ is a non-negative integer, and $\text{TOF}_{c_{25}}$ and $T_{c_{25}}$ are the TOF and period of the acoustic signal measured by the virtual hydrophone at $25°$C respectively. For $\text{TOF}_{c_{25}} < T_{c_{25}}$,

$$k = \text{round}\left[\frac{t_{c_{25},rx,n} - t_{c_{25},tx,0}}{T_{c_{25}}}\right] \tag{10}$$

And $d = \text{TOF}_{c_{25}} \cdot v_{25}$. Since Vemco hydrophones typically are calibrated to ± 20 parts per million [12] at $25°$C, for practical purposes it is safe to assume $v_{25} \approx v$, where v is the true sound velocity in water.

D. Summary and Algorithm Overview

Pseudocode for the algorithm is shown in Algorithm 1. $\vec{\theta}_t$ represents an array of past temperature data measured. Among the input parameters, $t_{c,rx,n}, \vec{\theta}_t$ are real-time measurements obtained from the hydrophone, and $t_{c,tx,0}, T_{c_{25}}$ needed to be obtained through calibration with the target tag. Notice that $t_{c,tx,0}$ equals $t_{c_{25},tx,0}$.

Algorithm 1 Temp-TOF: Distance Estimation with Non-linear Clock Skew Correction

function TEMP-TOF($t_{c,tx,0}, T_{c_{25}}, g(\theta), v, t_{c,rx,n}, \vec{\theta}_t, N$)
  $\theta(t) \leftarrow$ Non-linear fit with Levenberg-Marquardt method in the form $y = a + b\exp(cx)$ on $\vec{\theta}_t$ [17].
  $\Delta t_c \leftarrow t_{c,rx,n}/N$
  $t_{c_{25},rx,n} \leftarrow 0$
  for $i \leftarrow 0, N$ **do**
    $t_{c_{25},rx,n} \leftarrow t_{c_{25},rx,n} + g(\theta(i\Delta t_h))\Delta t_c$
  end for
  $k \leftarrow \text{round}\left[\frac{t_{c,rx,n} - t_{c,tx,0}}{T_{c_{25}}}\right]$
  $\text{TOF} \leftarrow t_{c_{25},rx,n} - (t_{c,tx,0} + kT_{c_{25}})$
  $d \leftarrow \text{TOF} \cdot v$
  return d
end function

V. Mixed-integer Linear Programming Algorithm for TDOA Estimation

TDOA measurements can be used to obtain angle measurements, and it requires time measurement data from both hydrophones. Clock drifts between hydrophones can therefore adversely affect the accuracy of TDOA measurements. While the algorithm presented in Section IV is suitable for distance estimation, the accuracy provided by the algorithm is not sufficient for TDOA estimation. As Section VII will show, the distance measurements have errors on the order of 1 m, which may not be low enough to to provide consistent TDOA measurements that are discernible by a pair of hydrophones mounted on an AUV.

To account for the relative clock skews between two boards, a MILP formulation is proposed. It estimates the most likely relative clock skew between the two hydrophones based on physical constraints of the hydrophone system.

A. Obtaining Angles from TDOA Data

TDOA measurements can be used to generate directional measurements by using the time difference between the two hydrophones. In particular, for a given TDOA, all possible signal locations are represented with a hyperbola, (see Fig. 2).

Assuming the acoustic signal's position can be expressed as (x, y) in a 2D Cartesian coordinate frame. The hyperbola representing all possible (x, y) can be expressed as

$$\frac{x^2}{\Delta d^2/4} - \frac{y^2}{D^2/4 - \Delta d^2/4} = 1 \tag{11}$$

where D is the separation between two hydrophones and $\Delta d = \text{TDOA}v$, where v is the sound speed [18]. The solution to Eq. (11) has asymptotes in the form of

$$y = \pm\sqrt{\frac{D^2/4 - \Delta d^2/4}{\Delta d^2/4}}x \tag{12}$$

Angle α shown in Fig. 2 can then be approximated by

$$\alpha = \begin{cases} \arctan\sqrt{\frac{D^2/4 - \Delta d^2/4}{\Delta d^2/4}} & \text{if } \Delta d \geq 0 \\ \pi - \arctan\sqrt{\frac{D^2/4 - \Delta d^2/4}{\Delta d^2/4}} & \text{otherwise} \end{cases} \tag{13}$$

B. MaxBound: Estimating Relative Clock Skews with a MILP Formulation

The relative clock skew between two hydrophones can be estimated using linear regression. However, linear least-square regression focuses only on minimizing the sum of squares of residuals; it does not consider the physical constraints of the system. Since the two hydrophones are separated by a fixed distance, the maximum possible TDOA value is the distance divided by sound speed. Using least-square regression, the corrected TDOA data might be greater than the maximum possible TDOA value.

A MILP formulation was developed to take physical constraints into account. In the formulation, V is the set of all TDOA values collected in a time interval. Parameters include

x_i	$i \in V$	time of measurement i
y_i	$i \in V$	uncorrected TDOA of measurement i
B		maximum possible TDOA
M		an arbitrarily large number

Variables include

d_i^+	$i \in V$	Positive distance y_i from the fitted line
d_i^-	$i \in V$	Negative distance y_i from the fitted line
b_0		Intercept of the fitted line
b_1		Slope of the fitted line
O_i	$i \in V$	Binary, 1 if $y_i - (b_0 + b_1 x_i) > B$

The objective function (Eq. (14)) aims to minimize the number of points violating the maximum possible TDOA.

$$\min \quad \sum_{i \in V} O_i \tag{14}$$

The constraints are listed below.

$$b_0 + b_1 x_i + d_i^+ - d_i^- = y_i \qquad \forall i \in V \tag{15}$$
$$d_i^+ - d_i^- - B \leq M O_i \qquad \forall i \in V \tag{16}$$
$$d_i^- - d_i^+ - B \leq M O_i \qquad \forall i \in V \tag{17}$$
$$b_0, b_1 \text{ unrestricted}$$
$$d_i^+, d_i^- \geq 0$$
$$O_i \in \{0, 1\}$$

Constraint (15) ensures b_0 and b_1 represent the intercept and slope. It also forces d_i^+ to take on non-zero values when the residual is positive, and d_i^+ to take on non-zero values when the residual is negative. Constraint (16) and (17) forces O_i to be 1 if and only if d_i^+ or d_i^- is greater than or equal to B. b_0 and b_1 can then be used to correct for relative clock skew between two hydrophones and obtain TDOA data. In the following section, this MILP formulation will be abbreviated as MaxBound.

C. Summary and Overview of the Algorithm

As discussed in Section IV, there exists significant non-linear clock skews. Assuming in a short period of time the relative clock skews are linear, Algorithm 2 uses a sliding-window approach to estimate the localized clock skews for each TDOA measurement, illustrated in Fig. 5. In addition, it keeps the old estimates of b_0 and b_1 until the objective function value (Eq. 14) exceeds a threshold.

In Algorithm 2, y_{new} and t_{new} are the value and time of the newest TDOA measurement. $b_{0,prev}$ and $b_{1,prev}$ are the most recent estimated fit parameters. $\vec{y}_{past}$ and $\vec{t}_{past}$ are the values and times of past TDOA measurements. D is the separation between hydrophones. v is the sound speed. W is the size of the sliding window. K is the maximum value of the objective function allowed until b_0 and b_1 need to be updated. The MILP solver used is Gurobi 7.5.2 [19]. For online processing, at least W data needs to be collected before starting the algorithm. For offline processing, the sliding window can be adjusted to center at each measurement.

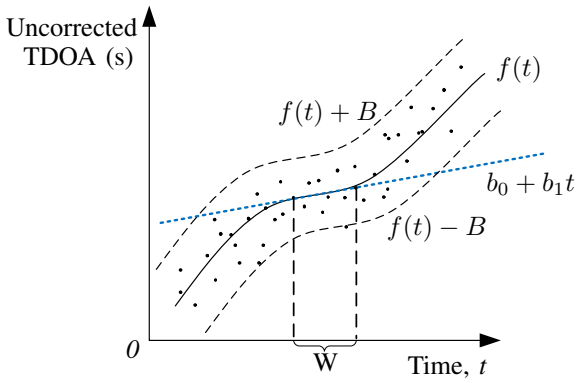

Fig. 5: $f(t)$ represents the clock skew difference between the two hydrophone clocks. The two dotted curves represent the maximum and minimum TDOA measurements given the skew. $b_0 + b_1 t$ represents the local clock skew function obtained by solving the MILP formulation over the window of size W.

Algorithm 2 MaxBound-TDOA: TDOA Estimation with MaxBound MILP Formulation

function MAXBOUND-TDOA(y_{new}, t_{new}, $b_{0,prev}$, $b_{1,prev}$, $\vec{y}_{past}$, $\vec{t}_{past}$, D, v, W, K)
  $B \leftarrow S/v$
  $\vec{t}, \vec{y} \leftarrow W$ most recent TDOA measurements combining t_{new}, y_{new}, $\vec{t}_{past}$, $\vec{y}_{past}$
  Calculate the objective function value $ObjVal$ with $\vec{t}, \vec{y}$ and $b_{0,prev}$, $b_{1,prev}$.
  if $ObjVal > K$ **then**
    $b_0, b_1 \leftarrow$ Solve MaxBound MILP Formulation with $\vec{t}$, $\vec{y}$ and B
  else
    $b_0, b_1 \leftarrow b_{0,prev}, b_{1,prev}$
  end if
  $y_{corrected} \leftarrow y_{new} - (b_0 + b_1 t_{new})$
  $\Delta d \leftarrow y_{corrected} \cdot v$
  $\alpha \leftarrow$ Calculated from Eq. 13 with D and Δd
  return α
end function

VI. Particle Filter

The location of the tag is estimated with a particle filter that fuses the TDOA and TOF measurements. The particle filter represents the belief state of the tag at time t with a set of particles $P_{tag,t}$ of size N_p. Each particle $p \in P_{tag,t}$ is represented by set $\{X_t^p w_t^p\}$. X_t^p represents the tag's position on a 2D Cartesian plane at time t and w_t^p represents the weight of the particle at time t. Upon initialization, $P_{tag,0}$ is populated with particles distributed uniformly across the map with equal weight. At each iteration, each particle is propagated randomly with Gaussian noise that has a standard deviation of σ and mean of 0. Given a valid measurement z which contains bearing z_α and distance z_d measurements from the TOF and TDOA, each particle p's weight is updated by first calculating the expected distance d_{exp}^p and

(a) Trial 1 Tracks

(b) Trial 2 Tracks

Fig. 6: Overhead view of the tracks in experiments conducted. AUV indicates the location of the AUV; Tag (GPS) indicates the location of the tag logged by the GPS receiver; Tag (PF) indicates the location of the tag estimated by the particle filter. Solid filled circles indicate the start of tracks, and + signs indicate the end of tracks.

the expected angle α^p_{exp}. Given the current state of the AUV X^{AUV}_t at a given time t, the expected angle can be calculated as:

$$\alpha^p_{exp} = \arctan\left(y_{X^p_t} - y_{X^{AUV}_t}, x_{X^p_t} - x_{X^{AUV}_t}\right) + \gamma \quad (18)$$

Similarly, the expected distance d can be obtained by calculating the Euclidean distance between X^{AUV}_t and X^p_t. Each particle's weight can then be updated with a Gaussian distribution function $W(z_s, s^p_{exp}, \sigma_s)$ given by

$$W(z_s, s^p_{exp}, \sigma_s) = \frac{1}{\sqrt{2\pi}\sigma_s} \exp \frac{-(z_s - s^p_{exp})^2}{2\sigma_s^2} \quad (19)$$

where z_s is a measurement, s^p_{exp} is the expected measurement and σ_s is the measurement standard deviation. After each prediction step, the particles are resampled systematically, and the location of the tag is calculated as the mean of $P_{tag,t}$. The entire process is outlined in Alg. 3.

Algorithm 3 Tag Position Estimator

for $p \in P_{tag,t}$ **do**
  // Propagate
  $X^p_t \leftarrow X^p_{t-1} + NormRandom(0, \sigma)$
  // Prediction
  if There are valid measurements z **then**
    $\alpha^p_{exp} \leftarrow Expected.Angle(X^{AUV}_t, X^p_t)$
    $d^p_{exp} \leftarrow Euclidean.Dist(X^{AUV}_t, X^p_t)$
    $w^p_t \leftarrow W(z_\alpha, \alpha^p_{exp}, \sigma_\alpha) * W(z_d, d^p_{exp}, \sigma_d)$
  else
    $w^p_t = w^p_{t-1}$
  end if
end for

// Correction
for $p \in P_{tag,t}$ **do**
  draw $p \in P_{tag,t}$ with probability w^p_t
  add p to $P_{tag,t+1}$
end for

TABLE I: Parameters used in Algorithm 1, 2 and 3

Temp-TOF	MaxBound-TDOA			Particle Filter			
N	D (m)	W	K	σ_α (rad)	σ_d (m)	σ (m)	N_p
1000	2.083	60	5	0.4	5	5	5000

VII. Experiments

Experiments were conducted at Big Fishermans Cove, Catalina Island, California to characterize the system's performance. For the experiments, an acoustic tag was hung from a boat equipped with a GPS receiver. The boat moved around in the cove while logging GPS positional data and time stamps. The AUV was simultaneously logging its GPS positional data and received acoustic tag signals. The acquired data was then downloaded and ran through an offline version of the localization system. The system's performance is then compared to those of two baseline methods: TOF without non-linear drift correction (abbreviated as Simple-TOF), and TDOA obtained with linear regression (abbreviated as LS-TDOA). Since the particle filter is non-deterministic, 100 trials were performed and errors were averaged. σ_α, σ_d and σ are determined experimentally. Table I summarizes the parameters used for Algorithm 1, 2 and 3.

A. Hardware System Overview

The acoustic tag used in the experiments was a Vemco 69 kHz V7 acoustic transmitter with a period of 7.767 s $\pm$ 0.001 s. The two VR2C 69 kHz hydrophones are separated by 2.083 m $\pm$ 0.003 m. The GPS receiver used was a Garmin eTrex 20 model, with a positional accuracy of 4 m.

B. Trial 1

Trial 1 started on August 11th, 2017 at 00:44 UTC time, and lasted about 10 minutes. Fig. 7a and 7b show the errors in distance measurements and angle measurements. Fig. 7c shows the particle filter localization errors. All the plots show that methods proposed in previous sections perform consistently better than the baseline methods.

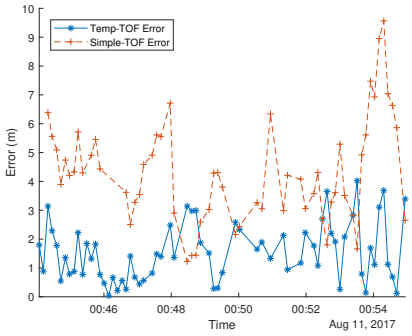

(a) Distance measurement errors of the purposed method (Temp-TOF) and baseline method (Simple-TOF).

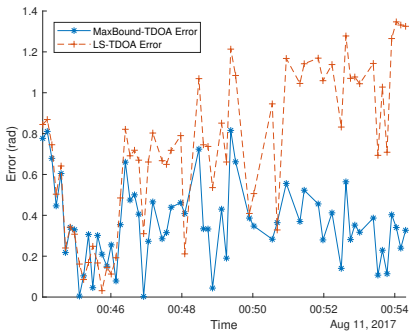

(b) Angle measurement errors of the purposed method (MaxBound-TDOA) and baseline method (LS-TDOA).

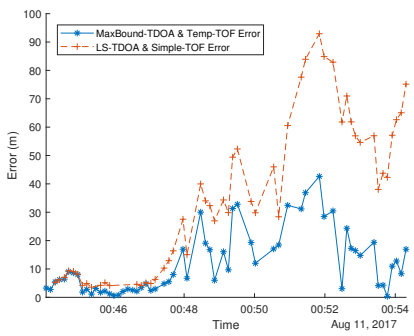

(c) Localization errors of the purposed method and baseline method.

Fig. 7: Trial 1 Results

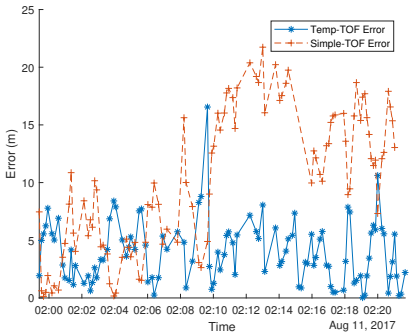

(a) Distance measurement errors of the purposed method (Temp-TOF) and baseline method (Simple-TOF).

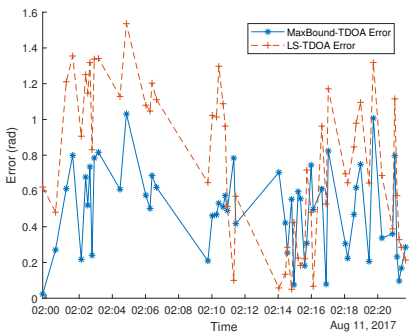

(b) Angle measurement errors of the purposed method (MaxBound-TDOA) and baseline method (LS-TDOA).

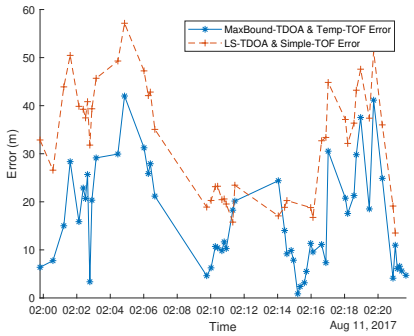

(c) Localization errors of the purposed method and baseline method.

Fig. 8: Trial 2 Results

C. Trial 2

Trial 2 started on August 11th, 2017 at 02:00 UTC time, and lasted about 20 minutes. Fig. 8a and 8b show the errors in distance measurements and angle measurements. Fig. 8c shows the particle filter localization errors. Similar to the plots for Trial 1, methods proposed in previous sections perform better than the baseline methods.

D. Results

Table II, III and IV show a summary of some important statistics of the experiments' results. For the mean angle measurement errors, MaxBound-TDOA achieves an average reduction of 43% comparing to using LS-TDOA method for Trial 1 and 2, and a reduction of 18% comparing to the 30° (0.52 rad) mean angle measurement error demonstrated in [2] using synchronized hydrophones.

For the mean distance measurement errors, Temp-TOF achieves a reduction of 57% for Trial 1 and 2. For the Simple-TOF method, 4% of distance measurements in Trial 1 and 8% in Trial 2 are removed because their values are on the order of 10^4 meters, which far exceeds the possible range of the hydrophones. None of the TOF measurements calculated by Temp-TOF is removed. On average, the proposed system achieved a localization error of 14 m with a standard deviation of 11 m, comparable to the positional errors obtained in [2]. Comparing to the baseline methods, the proposed system reduced mean localization error by 59% and standard deviation by 44%.

TABLE II: Distance measurements errors of the two trials using temperature correction, comparing to ToF method without temperature correction

	Trial 1		Trial 2	
	Simple-TOF	Temp-TOF	Simple-TOF	Temp-TOF
Mean Err. (m)	4	2	10	4
Median Err. (m)	4	1	10	4
SD Err. (m)	2	1	6	3

TABLE III: Angle measurements errors of the two trials using MILP, comparing to linear regression drift correction.

	Trial 1		Trial 2	
	LS-TDOA	MaxBound-TDOA	LS-TDOA	MaxBound-TDOA
Mean Err. (rad)	0.72	0.36	0.77	0.49
Median Err. (rad)	0.72	0.34	0.77	0.51
SD Err. (rad)	0.37	0.19	0.42	0.25

TABLE IV: State estimation positional errors of the two trials using MILP and temperature correction, comparing to baseline method.

	Trial 1		Trial 2	
	Simple-TOF + LS-TDOA	Temp-TOF + MaxBound-TDOA	Simple-TOF + LS-TDOA	Temp-TOF + MaxBound-TDOA
Mean Err. (m)	35	12	33	16
Median Err. (m)	32	8	34	13
SD Err. (m)	27	11	12	11

VIII. Conclusion and Future Works

Experimental results show that Algorithm 1 is capable of reducing the effects of non-linear drift and reducing the TOF range measurement error by a significant margin. Algorithm 2 is capable of reducing the TDOA error significantly from a naive linear fit of the clock differences. Overall, the localization system is able to achieve a localization error comparable to that shown in [2] with two synchronized hydrophones. This paper makes several contributions in the future of marine animal tracking with AUVs, including: 1) a novel mixed integer programming approach that dynamically accounts for clock skew between two clock 2) a new temperature based calibration method for non-linear drift, and lastly 3) an inexpensive way for researchers to incorporate off the shelf unsynchronized sensor systems with AUVs.

Future works for this project include using temperature-dependent sound velocities in calculations, and conducting longer experiments to further validate the effectiveness of the system in real time tracking. Another extension of this work is the application of the localization system to existing passive acoustic tracking arrays.

Acknowledgments

Field experiments detailed in this work were performed at the USC Wrigley Institute for Environmental Studies. Preliminary testing of the system was conducted at the Robert J. Bernard Biological Field Station.

References

[1] Y. Lin, H. Kastein, T. Peterson, C. Clark, C. White, and C. Lowe, "Using Time of Flight Distance Calculations for Tagged Shark Localization with an AUV," in *Unmanned Tethered Submersible Technology*, 2013.

[2] Y. Lin, J. Hsiung, R. Piersall, C. White, C. G. Lowe, and C. M. Clark, "A Multi-Autonomous Underwater Vehicle System for Autonomous Tracking of Marine Life," *Journal of Field Robotics*, vol. 34, no. 4, pp. 757–774, 2017.

[3] T. Grothues and J. Dobarro, "Fish telemetry and positioning from an autonomous underwater vehicle (AUV)," *Instrumentation viewpoint*, vol. 08087, no. 609, pp. 78–79, 2009. [Online]. Available: http://dialnet.unirioja.es/servlet/articulo?codigo=3204780

[4] G. A. Warner, S. E. Dosso, and D. E. Hannay, "Bowhead whale localization using time-difference-of-arrival data from asynchronous recorders," *The Journal of the Acoustical Society of America*, vol. 141, no. 3, pp. 1921–1935, mar 2017. [Online]. Available: http://aip.scitation.org/doi/10.1121/1.4978438

[5] H. Baktoft, K. Ø. Gjelland, F. Økland, and U. H. Thygesen, "Positioning of aquatic animals based on time-of-arrival and random walk models using YAPS (Yet Another Positioning Solver)," *Scientific Reports*, 2017.

[6] M. S. Sim, B.-K. Choi, B.-N. Kim, and K. K. Lee, "Underwater acoustic source localization using closely spaced hydrophone pairs," *Japanese Journal of Applied Physics*, vol. 55, no. 7S1, p. 07KG05, jul 2016.

[7] S. Zhu, N. Jin, L. Wang, X. Zheng, S. Yang, and M. Zhu, "A novel dual-hydrophone localization method in underwater sensor networks," in *2016 IEEE/OES China Ocean Acoustics (COA)*. IEEE, jan 2016, pp. 1–4. [Online]. Available: http://ieeexplore.ieee.org/document/7535787/

[8] N. R. Rypkema, E. M. Fischell, and H. Schmidt, "One-way travel-time inverted ultra-short baseline localization for low-cost autonomous underwater vehicles," in *Proceedings - IEEE International Conference on Robotics and Automation*, 2017, pp. 4920–4926.

[9] J. V. Hook, P. Tokekar, E. Branson, P. G. Bajer, P. W. Sorensen, and V. Isler, "Experimental Robotics," vol. 109, pp. 859–873, 2016. [Online]. Available: http://link.springer.com/10.1007/978-3-319-23778-7

[10] S. Shatara and X. Tan, "An efficient, time-of-flight-based underwater acoustic ranging system for small robotic fish," *IEEE Journal of Oceanic Engineering*, vol. 35, no. 4, pp. 837–846, Oct 2010.

[11] M. Espinoza, T. J. Farrugia, D. M. Webber, F. Smith, and C. G. Lowe, "Testing a new acoustic telemetry technique to quantify long-term, fine-scale movements of aquatic animals," *Fisheries Research*, 2011.

[12] F. Smith, "Understanding HPE in the VEMCO Positioning System (VPS)," Bedford, 2013. [Online]. Available: http://vemco.com/wp-content/uploads/2013/09/understanding-hpe-vps.pdf

[13] M. Frerking, *Crystal Oscillator Design and Temperature Compensation*. Springer Netherlands, 2012. [Online]. Available: https://books.google.com/books?id=SXciCQAAQBAJ

[14] B. Sterzbach, "GPS-based Clock Synchronization in a Mobile, Distributed Real-Time System," *Real-Time Systems*, vol. 12, no. 1, pp. 63–75, 1997. [Online]. Available: http://link.springer.com/10.1023/A:1007910115824

[15] R. Baker and I. Martinovic, "Secure Location Verification with a Mobile Receiver," *Proceedings of the 2nd ACM Workshop on Cyber-Physical Systems Security and Privacy - CPS-SPC '16*, pp. 35–46, 2016. [Online]. Available: http://dl.acm.org/citation.cfm?doid=2994487.2994497

[16] P. Marchetto, A. Strickhart, R. Mack, and H. Cheyne, "Temperature compensation of a quartz tuning-fork clock crystal via post-processing," *2012 IEEE International Frequency Control Symposium, IFCS 2012, Proceedings*, pp. 332–335, 2012.

[17] W. H. Press, S. A. Teukolsky, W. T. Vetterling, and B. P. Flannery, *Numerical recipes in C : the art of scientific computing*. Cambridge University Press, 1992. [Online]. Available: https://dl.acm.org/citation.cfm?id=148286

[18] F. Gustafsson and F. Gunnarsson, "Positioning using time-difference of arrival measurements," *2003 IEEE International Conference on Acoustics, Speech, and Signal Processing, 2003. Proceedings. (ICASSP '03).*, vol. 6, pp. 553–556, 2003.

[19] I. Gurobi Optimization, "Gurobi optimizer reference manual," 2016. [Online]. Available: http://www.gurobi.com